Bi-Fi: An Embedded Sensor/System Architecture for Remote Biological Monitoring

Shahin Farshchi, *Student Member, IEEE*, Aleksey Pesterev, Paul H. Nuyujukian, Istvan Mody, and Jack W. Judy, *Senior Member, IEEE*

***Abstract*—Wireless-enabled processor modules intended for communicating low-frequency phenomena (i.e., temperature, humidity, and ambient light) have been enabled to acquire and transmit multiple biological signals in real time, which has been achieved by using computationally efficient data acquisition, filtering, and compression algorithms, and interfacing the modules with biological interface hardware. The sensor modules can acquire and transmit raw biological signals at a rate of 32 kb/s, which is near the hardware limit of the modules. Furthermore, onboard signal processing enables one channel, sampled at a rate of 4000 samples/s at 12-bit resolution, to be compressed via adaptive differential-pulse-code modulation (ADPCM) and transmitted in real time. In addition, the sensors can be configured to filter and transmit individual time-referenced "spike" waveforms, or to transmit the spike height and width for alleviating network traffic and increasing battery life. The system is capable of acquiring eight channels of analog signals as well as data via an asynchronous serial connection. A back-end server archives the biological data received via networked gateway sensors, and hosts them to a client application that enables users to browse recorded data. The system also acquires, filters, and transmits oxygen saturation and pulse rate via a commercial-off-the-shelf interface board. The system architecture can be configured for performing real-time nonobtrusive biological monitoring of humans or rodents. This paper demonstrates that low-power, computational, and bandwidth-constrained wireless-enabled platforms can indeed be leveraged for wireless biosignal monitoring.**

***Index Terms*—Brain–Machine interface, mote, neural recording, smart dust, spike compression, spike filtering, stimulation, telemetry, TinyOS, wireless.**

I. Introduction

A MAJOR challenge to realize a remote biological-monitoring system is the creation of miniature wireless biological sensors that serve as the interface between the patient and the network infrastructure. These wireless biological sensors must be capable of sensing, amplifying, and transmitting biological signals that range from the order of tens of microvolts to several milivolts, while being nonobtrusive (i.e., compact) and consuming low power (i.e., sufficient battery life). The vast majority of the power used by the wireless sensor is dedicated to the radio transmitter for signal transmission. Therefore, the addition of local data-processing capabilities can prolong battery life significantly, due to the elimination of the requirement for constant high-throughput wireless data transmission. In addition, the combination of onboard signal-processing capabilities and a receiver can enable user-defined multimode operation, such as allowing the observer to switch between low-power event detection and variable rates of real-time biological-signal transmission. Therefore, a system that combines bidirectional communications with onboard computational abilities would be superior to a simple transmitter/receiver unit. Possible approaches for implementing a wireless biological sensor range from assembling commercial-off-the-shelf PC (COTS-PC) components [1] to custom-fabricating integrated circuits (ICs) [2]. COTS-PC components yield large power-intensive units with powerful communications and signal-processing capabilities, while custom ICs yield very specialized, compact, and power-efficient solutions. Unfortunately, investing in the development of custom ICs for digital signal acquisition, processing, and communication for nonstandardized applications (e.g., biological-signal recording), unlike cellular phones that operate on strict international standards (e.g., GSM, Bluetooth, etc.) may not be economically feasible. The overlay of a biological-recording system upon an embedded wireless sensing and communications platform has been reported in [3]. This wireless communications platform uses ultraminiature computers as sensor nodes (sometimes referred to as "motes"), which are capable of digital-signal processing and two-way wireless communication. The significance of this paper is that it is a novel attempt to enable a mote to communicate neural signals in real time, which is an application that requires the mote to operate at or near the hardware limit, as opposed to other approaches that use hardware with high degree of communications and digital-signal-processing capabilities that are not fully utilized, at the expense of unnecessary power consumption. The motes operate on a component-based operating system called TinyOS [4]. The TinyOS-based motes (i.e., MICA2) have been used as a foundation for an electroencephalograms (EEG) recording system that is capable of transmitting up to six channels of EEG at an aggregate rate of up to 2400 8-bit samples/s (1200 8-bit samples/s for the MICA2DOT) among all channels. The system was later enhanced by using a later generation of motes (the MICAz) and TinyOS build and is capable of capturing and transmitting neural signals at a rate of 45 kb/s for a single channel of spike recording at approximately 5600 samples/s or eight channels of EEG [4]. Unfortunately, the high power consumption required to continuously sample and transmit data-limited battery life to approximately 5 h [5] . This paper leverages the direct memory access (DMA) capability offered in the more modern TelosB mote platform to expand on

Manuscript received July 26, 2006; revised February 9, 2007.

S. Farshchi, P. H. Nuyujukian, A. Pesterev, and J. W. Judy are with the Department of Electrical Engineering, University of California at Los Angeles, Los Angeles, CA 90025 USA (e-mail: shahin@ee.ucla.edu).

I. Mody is with the Department of Neurology, University of California at Los Angeles, Los Angeles, CA 90025 USA (e-mail: mody@ucla.edu).

Digital Object Identifier 10.1109/TITB.2007.897600

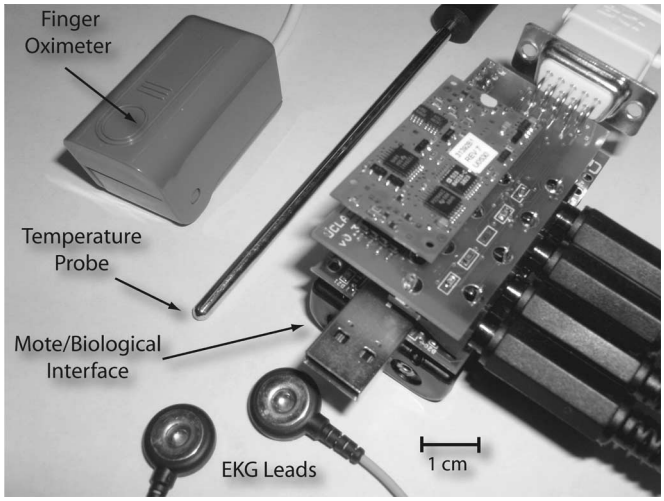

Fig. 1. Bi-Fi Mote, including the Smiths Medical PM.3044 finger oximeter, Erlich Senser SS TM10 thermistor, and Discount Disposables TD429 EKG leads.

the previous work reported in [3] and [5] by: 1) adding signal-processing capabilities to lower bandwidth, hence, increasing battery life and 2) pulse oximetry and temperature sensing. The wireless sensor (depicted in Fig. 1) combines a TelosB mote with biological interface circuitry and probes, thus, yielding a matchbox-sized form factor.

Biological signals of interest include temperature, local-field potentials (LFP), and electrocardiograms (EKG). In addition, spike identification is required for many brain–computer-interface (BCI) applications [6]. Furthermore, the system must be capable of bidirectional communications to enable remote configuration of the sensor (e.g., adjustable gain and recording bandwidth) that is embedded on the patient or test subject. Remote system configurability enables the investigator to achieve a compromise between the granularity of the received information and battery life, as the radio is the largest power-consuming component of the device. For example, transmitting a patient's vital signs (EKG, pulse oximetry, and temperature) in real time results in a battery life of 100 h from a pair of AA alkaline batteries. The telehealthcare provider could choose to have the sensor evaluate vital-sign data locally to arrive at a modified early warning score (MEWS) [7], which is transmitted periodically (e.g., hourly, weekly, monthly, etc.), or only in the event that there is a change in calculated score, which requires the system to be recharged approximately once every ten weeks (as microcontroller power dissipation dominates in this mode of operation). Brain–computer-interface developers desire a record of the time at which neural spikes occur and an identification of the cells from which they originate, which enables dual-channel recording and results in a battery life of approximately three days from a single 3-V coin cell [5]. Neuroscientists may not desire any sort of filtering to be performed whatsoever in order to have a record of the actual electrophysiological signal, requiring a constant data sampling and transmission rate of 32 kb/s for a single channel, which results in a battery life of approximately 5 h from a coin cell [5].

II. Definition of a New Approach

A. Existing Miniature-Scale Wireless Biosignal-Monitoring Systems

A thorough review of existing approaches toward developing wireless biological sensors has been covered in [5]. These approaches can be divided into two major categories: fully analog and microcontroller-based. Fully analog systems are either: 1) fully integrated amplifiers and transceivers or 2) assembled multichip modules. Although the fully integrated devices demonstrated in [2], [8]–[10], and feature very small size (5–100 mm) and low power consumption (approximately 2–14 mWs), they do not provide digital-signal filtering or bidirectional communications (except for the system described in [10], which can modulate the inductive power link as a carrier signal for communication from the base station to the sensor). In addition, large reintegration efforts could be required for even minor upgrades and improvements (e.g., channel count, signal bandwidth, etc.). The assembled multichip modules, which are composed of COTS ICs for the amplifier and the transmitter (i.e., [11]–[13]), have performance characteristics similar to those that use custom ICs, but have a much shorter development time, greater size, more mass, and increased power consumption. In order to compare the performance and capabilities of the fully analog systems, it would be useful to define a figure of merit as the analog-telemetry-efficiency factor (ATEF)

$$\text{ATEF} = \frac{BW\, d}{mP} \tag{1}$$

where BW is the aggregate communications bandwidth (expressed in kilohertz), d is the maximum telemetry distance (expressed in meters), m is the mass of the sensor (expressed in grams), and P is the average power dissipation (expressed in miliwatts). Table I presents several recently reported fully analog biological sensors and compares them on the basis of the ATEF figure of merit. Although a microcontroller-based system with ample signal-processing and bidirectional-communications abilities has been demonstrated [14], its size, weight, and power consumption is significantly greater than the aforementioned integrated systems. Other microcontroller-based systems have been introduced [15]–[17]; however, their data throughput and processing performance were not near the potential limits of their underlying hardware (i.e., they do not perform digital-signal filtering). The underutilization of such powerful hardware leads to unnecessarily high power consumption, which will be outlined in Sections VI and VII. In order to compare the performance and capabilities of the microcontroller-based systems, it would be useful to define a figure of merit as the digital-telemetry-efficiency factor (DTEF)

$$\text{DTEF} = \frac{BR_{\text{eff}}\, d}{mP} \tag{2}$$

where BR_{eff} is the effective bitrate (expressed in bits per second) that takes into account any form of compression (e.g., a compression efficiency of 2 will double the effective bitrate), d is the maximum telemetry distance (expressed in meters), m is the mass of the sensor (expressed in grams), and P is the average

TABLE I
COMPARISON WITH FULLY ANALOG SYSEMS

Institution	UCLA	Michigan	Aachen	Tokyo U.	UCLA	Clev. Med.
Number of Analog Channels	8	7	2	1	1	8
Telemetry Link Freq (MHz)	2400	94-98	88-108	80-90	3200	902- 928
Modulation Scheme	DSSS/O-QPSK	TDMA/Analog FM	FM Stereo	Analog FM	Analog FM	FSK
Power Supply	3 V	±1.5 V	±1.4 V	3 V	Inductive	9 V
Max. Power Dissipation	97 mW	~ 2.05 mW	-	10 mW	13.8 mW	-
Transmission Range	9 meters	a few meters	a few meters	~16 m	< 1 meter	< 46 m
Sensitivity	1 - 15 mV	0.1 - 5 mV	-	-	0.015-15 mV	-
Total Bandwidth	4 kHz	10 kHz	-	-	10 kHz	-
Dimensions (cm)	6.5 × 3.1 × 1.5	0.22 × 0.22	2.5 × 1 × 0.5	1.5 × 0.8	0.5 × 0.5 × 1	6.4 × 5.1 × 1
Total Weight (w/ battery)	66 gr	> 1.1 g	> 3.1 g	> 0.1 g	< 1 g	> 68 g
ATEF	0.005623	7.32 (1-gr batt assumed)	*Insufficient data*	*Insufficient data*	0.72	*Insufficient data*
Reference	*This Work*	*[9]*	*[11]*	*[12]*	*[2]*	*[13]*

TABLE II
COMPARISON WITH MICROPROCESSOR-BASED SYSTEMS

Institution	UCLA	NASA	Kansas State	Lboro	Harvard	Duke
Number of Analog Channels	8	10	5	8	2	12
Communication Standard	ZigBee	BT	BT	BT	ZigBee	802.11b
Processor	8-MHz TI	7.37-MHz PIC	25-MHz PIC	40-MHz AMD	8-MHz TI	66-MHz AMD
On-Board Memory (bytes)	1 M	32 M	2 M	256 k	1 M	
Power Supply	3 V	3 V	6 V	9 V	3 V	3.3 V and 5 V
Power Dissipation (streaming)	97 mW	360 mW	3.44 W	4.5 W	~ 100 mW	4.0 W
Transmission Range	9 meters	10 meters	-	-	9 m	9 m
Signal Interpretation	Neural Spike	-	-	-	-	-
Total Bandwidth	4 kHz	~300 Hz	250 Hz	-	120 Hz	31.25 kHz
Dimensions (cm)	6.5 × 3.1 × 1.5	12.9 × 10 × 0.2	-	-	5.8 × 3.2	5.1 × 8.1 × 12.4
Total Weight (w/ battery)	66 gr	166 gr	-	-	~ 66 gr	235 g
DTEF	0.06748	0.0006024	*Insufficient data*	*Insufficient data*	0.001309	0.04309
Reference	*This Work*	*[15]*	*[17]*	*[16]*	*[36]*	*[1]*

power dissipation of the sensor (expressed in miliwatts). Table II presents several recently reported microcontroller-based biological sensors and compares them on the basis of the DTEF figure of merit.

B. TinyOS and the Mica-Based Sensor Network

The type of mote used in this paper is the TelosB mote produced by Crossbow Technology, Inc. (San Jose, CA, USA) and Moteiv (El Cerrito, CA, USA). Data is processed by a microcontroller (MSP430, Texas Instruments, Dallas, TX, USA) with 10 kB of RAM. The TI MSP430 has eight analog input channels that are time-multiplexed onto a single analog-to-digital converter (ADC). Data transmission is handled by a ZigBee-compliant (IEEE 802.15.4) 2.4-GHz transceiver (Chipcon CC2420, Oslo, Norway). An antenna embedded on the printed-circuit board is used for wireless communication. When two 1.5-V batteries (Panasonic Industrial AA, Secaucus, NJ, USA) are installed, the TelosB mote becomes approximately the size of a matchbox (65 mm × 31 mm ×21 mm). Users have the option of using more compact 3-V batteries that may be more suitable for their application (e.g., coin cells for experiments involving rodents). One TelosB mote, running a signal acquisition, filtering, and transmission framework [18], has been interfaced with the test subject via a biological interface (depicted in Fig. 1). A second TelosB mote interfaced with a gateway module, which in this experiment is a laptop (Thinkpad X21, IBM, Armonk, NY, USA) running a modified version of Emstar [19] to emulate a Stargate Gateway (Crossbow Technology, Inc.), wirelessly receives and forwards sensor readings over the network (Ethernet). The gateway module also provides sensors with configuration data for remote adjustment of filter properties. This paper has been directed toward investigating software filters, biological interfaces, and a back-end server architecture to enable chronic, multichannel, and wireless biosignal recording.

III. SYSTEM DESIGN

A. Hardware

Two types of biological interface circuits are used in this paper. For capturing raw EEG, an instrumentation amplifier (AD627, Analog Devices Norwood, MA, USA) is used. The AD627 is preceded by a high-pass filter with its f-3dB point set to 1 Hz, followed by a low-pass filter with its f-3dB point set to 200 Hz. The gain of the AD627 is set by an external resistor to 200. This circuit has been described in greater detail in [5]. A three-lead EKG circuit has been implemented with an instrumentation amplifier (INA321, Texas Instruments) and a quad op-amp (OPA4336, Texas Instruments). The details of this circuit layout can be found in the INA321 datasheet. The outputs of these circuits are interfaced directly with the ADC inputs of the TelosB mote. For capturing oxygen saturation and pulse rate, an oximeter (Smiths Medical PM 31392B1, Waukesha, WI, USA) is interfaced with the serial input on the TelosB (UART0) in a manner similar to [20], albeit with a TelosB rather than a MICAz mote. Temperature sensing is performed with the temperature sensor thermistor (Senser SS TM10, Erlich

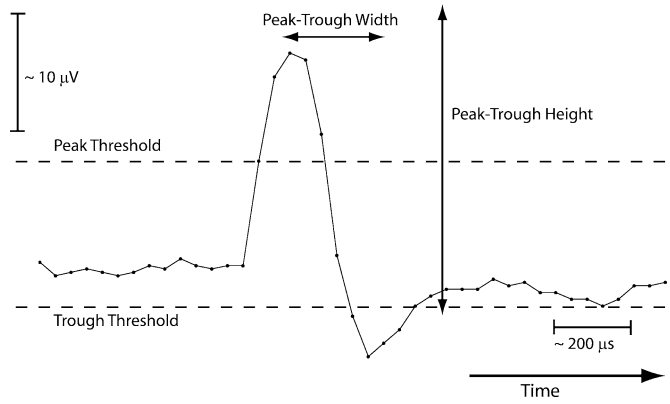

Fig. 2. Neural-spike parameters of interest (adapted from [21]).

Industrial Development Corporation, Charlotte, NC, USA) as part of a resistor bridge circuit followed by an INA321 instrumentation amplifier. Although the present form factor of the temperature probe is not suitable for biological temperature sensing, a thermistor with a more suitable form factor could be used in its place and would only require different resistor values in the resistive bridge sensing circuit.

B. Software

To best leverage the limited processing capabilities of the TelosB for the purpose of improving battery life, computationally efficient filters were designed for acquiring neural spikes to minimize the amount of raw data being transmitted from the radio while still providing useful biological information. These filters were incorporated as part of a modular framework for signal acquisition, filtering, and transmission. The framework operates at the hardware level, thus minimizing overhead and achieving the maximum performance that can be provided by the direct memory access (DMA)-enabled microcontroller and radio. Details regarding this framework are beyond the scope of this paper, and can be found in [18]. An excellent example of where sensor-level signal processing can yield high bandwidth and, hence, power savings is detecting and classifying single-neuron firings when investigating single-unit activity. Raw neural recording and transmission normally requires a bandwidth in excess of 40 kb/s per channel [21]. Numerous methods have been investigated for detecting a neural spike (or discharge of a single neuron) to ease network traffic and bandwidth requirements. The memory and computational resources required by each spike-detection algorithm vary from requiring powerful desktop PCs [22] to simple analog circuits [23]. Obeid and Wolf [14] have performed an evaluation of neural-spike-detection algorithms, and concluded that for systems with limited computational resources, taking the absolute value of the neural signal before applying a threshold (in combination with a refractory period) is just as effective as applying more elaborate energy-based detectors. In addition, basic spike sorting can be achieved by measuring the width and height of each individual spike waveform [21]. The spike features that neuroscientists use to categorize the spikes are illustrated in Fig. 2.

For detecting the spikes, an adaptive spike-detection algorithm is used to detect neural spikes in the presence of varying background noise [24]. This approach avoids the occurrence of false positives due to occasional increases in background noise power. If the baseline level of the high-pass filtered neural signal is regarded as band-limited white Gaussian noises, then the probability of exceeding a threshold set at one standard deviation, or root mean square (rms) of the baseline is 15.9%. Setting the threshold at three standard deviations of the baseline noise level results in spikes being detected reliably without false positives, as Gaussian noise rarely exceeds three times its rms value. The lowest multiple of standard deviations of the baseline at which the threshold can be set depends on the signal-to-noise ratio (SNR) of the spike waveform. An in-depth analysis of spike-detection effectiveness as a function of threshold and SNR for absolute-threshold-based spike-detection algorithms has been presented in [14].

The algorithm continuously buffers the signal until its absolute value exceeds a user-defined number of standard deviations of the baseline noise, which is calculated via a sliding-window algorithm or a user-defined threshold. To avoid interference (such as movement artifacts) from being classified as neural spikes, the height, width, and trough depths of the detected spike (see Fig. 2) are also measured against a range of acceptable values predetermined by the user. If the measured spike parameters fit within these ranges, the spike is accepted by the filter. The data points representing the spike are compressed via adaptive differential-pulse-code modulation (ADPCM) [25] and marked for transmission over the radio. This filtering method provides users with a time-reference record of the individual spike waveforms. A second filter passes the height and width of each spike along with its time of occurrence, which enables the client to statistically categorize the spikes based on their features [21].

EKG-feature extraction has been recently attempted on embedded sensors for sensor-level analysis [26], using a modified version of the real-time QRS-detection algorithm [27] in simulation. Implementing feature-detection algorithms as well as a classifier [28] would enable the TelosB mote to detect various types of arrhythmia. This capability would eliminate the need for sending the real-time EKG signal, and only require the sensor to transmit information regarding an arrhythmia if one should be detected. However, in the present system, the raw waveform is simply compressed by ADPCM and transmitted over the radio. EKG feature extraction and classification will be investigated in future work. Local-field potentials are rhythmically varying electrical impulses of large neural populations that vary at rates below 100 Hz [29]. Local-field potential energy has been correlated to specific arm movement and reach parameters such as direction, distance, and speed [30]. The energy of the signal is derived by obtaining its rms value over a user-programmable window. For calculating the square root in a computationally efficient manner, a lookup-table-based algorithm has been employed that only uses bit-shifting for the square-root computation. The 31392B1 pulse oximeter transmits 60 4-byte packets/s via its serial connection. The packets contain pulse rate and blood oxygen saturation, both digitized

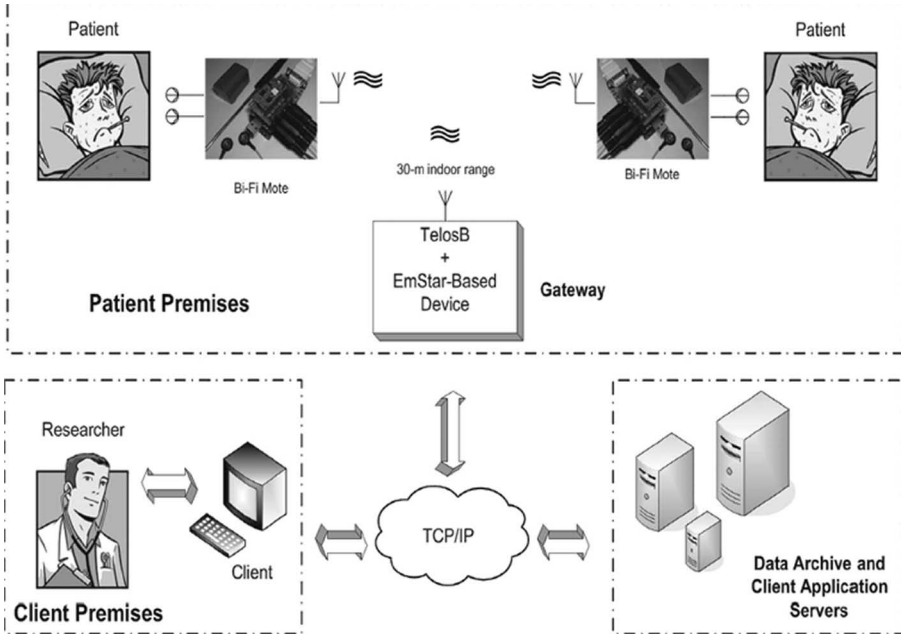

Fig. 3. Bi-Fi system architecture.

by default at 8-bit resolution. A TinyOS software component has been written to interface the TelosB mote to the 31392B1. A software filter averages oxygen saturation and pulse-rate readings, and transmits them in the form of 2 bytes over a user-defined period of time. Oxygen saturation and pulse-rate readings can be transmitted only when they differ by a relative percentage, which is programmable by the user. The Chipcon CC2420 radio on the TelosB uses the TI MSP430-UART0 bus for configuration, which prevents the UART0 from being used by a peripheral device (such as the 31392B1). A bus arbitrator has been implemented under TinyOS that allows the bus to be used by the 31392B1 when the TelosB is prepared to acquire data from it. The arbitrator then returns the bus to the radio when the data required from the 31392B1 has been received. Data transmission takes place in packet format. The type of signal (e.g., pulse-rate, oxygen saturation, neural signal, or temperature), signal resolution, filter type, and a time reference are included in the packet header. An overall system-level diagram is depicted in Fig. 3, which illustrates the flow of data through the system. The transmitted data is received by a second TelosB mote that is interfaced with the Emstar-enabled laptop. The gateway module parses the data from the received packets, and encapsulates them as structured query language (SQL) queries for posting to the archive server. The SQL queries are transmitted via TCP/IP to the archive server. The archive server is a Linux-based system running a database server (MySQL, MySQL AB, Uppsala, Sweden). A Java-enabled client application for use on a desktop PC has been designed to browse the biological data from the archive server over a network connection. The client application reconstructs raw waveforms by applying an eighth-order Chebyshev filter to an up-sampled version (by a factor of 10) of the original archived waveform.

IV. System Testing

For neural recording, the Bi-Fi system can be interfaced directly with a rodent via an implanted depth electrode as illustrated in [3] and [5], which demonstrate real-time wireless neural-signal recording with the TinyOS-based embedded sensors. For testing the spike-filtering characteristics of the system, an arbitrary-waveform generator (33120A, Agilent Technologies, Inc., Palo Alto, CA, USA) was programmed with prerecorded spike datasets. The data was originally acquired *in vivo* from freely moving rats using five four-channel MOSFET-input operational amplifiers mounted in the cable connector to remove movement artifacts. Data were recorded wideband (0.1 Hz–5 kHz) and sampled at 10 kHz/channel (16 channels) with 12-bit precision. Spikes were obtained by applying a high-pass filter with a f-3-dB frequency of 300 Hz. The signal generator was programmed to output the 1-s 10 000-point dataset with 12-bit precision (over a 50-mV peak-to-peak dynamic range, resulting in an accuracy of approximately 12 V, with each point connected by a straight line segment) at a rate of 1 Hz. Since the precision and data rate of the waveform generator is identical to those of the sampled signal, no signal information was lost. The ability of the system to measure pulse rate and oxygen saturation was tested by attaching the finger oximeter (Smiths Medical PM 3044) to the index finger of a human test subject.

V. Results

A. Neural Recording

Fig. 4(a) displays the original dataset acquired from an oscilloscope, which was attached to the output of the signal generator programmed to output the spike waveforms. Fig. 4(b) displays the dataset that was acquired and transmitted by the TelosB

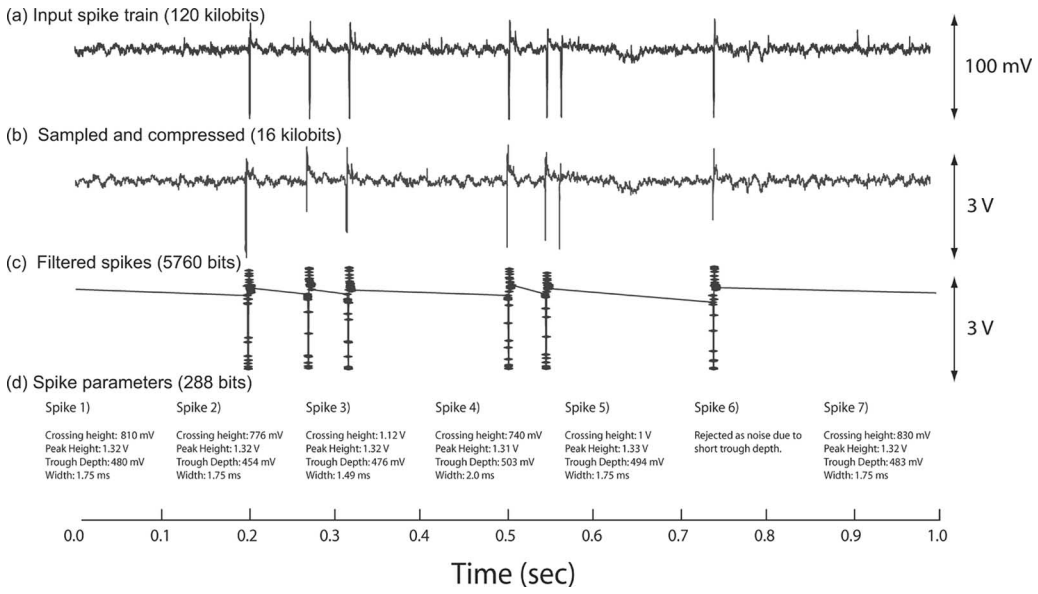

Fig. 4. Neural signal (a) applied to the mote, (b) ADPCM-compressed, (c) filtered waveforms, (d) spike parameters, and the bandwidth required for transmitting them. To demonstrate the ability of the filter to accept spikes while rejecting unwanted noise (such as motion artifacts, which result in spike-like patterns in the input signal), the filter parameters (i.e., window of acceptable spike heights, widths, and trough depths, which are user programmable) were programmed to reject the sixth-spike waveform in the dataset—as though it were noise—as it has a very low trough depth.

mote at 4000 12-bit samples/s followed by ADPCM compression. Fig. 4(c) displays the transmitted signal when the mote was programmed to acquire the neural signal at 8000 12-bit samples, and then to detect and transmit time-referenced spikes using an adaptive absolute-value-thresholding algorithm. The algorithm sets two thresholds (one positive and one negative) that are defined by the user as multiples in the rms value of the baseline noise. In the event of a positive-threshold crossing, the algorithm anticipates a negative-threshold crossing within a user-defined period of time (set to 500 s). If a negative-threshold crossing occurs in this time window, the time at which the spike occurred, as well as its data points (or the peak-trough height and peak-trough width, depending on the mode of operation) are recorded and marked for transmission over the radio. This algorithm is discussed in greater detail in [31]. To illustrate the ability of the filter to accept spikes in the present of unwanted noise (such as motion artifacts, which could result in signals that resemble spikes), the filter parameters were chosen such that the required signal-trough depth exceeded that of the sixth spike; hence, the spike was rejected as though it were unwanted noise. The signal parameters extracted from the spike waveform are listed in Fig. 4(d). The amount of data throughput necessary for transmitting each waveform is also labeled in Fig. 4. Transmitting the spike parameters only (e.g., spike time, peak height, and trough depth) requires only 48 bits per spike, thus, lowering the required bandwidth for transmitting the 1-s signal to only 288 bits. The normalized correlation of the received ADPCM-compressed raw spike signal to the autocorrelated original waveform is over 99%.

B. Pulse Oximetry and Heart Rate

Transmitting the raw heart-rate and pulse-oximetry signals would require a total data rate of 1.92 kb/s. However, programming the TelosB mote to only transmit the heart rate and pulse oximetry when heart rate varies by 5 beats/min, or when oxygen saturation changed by 2%, can significantly lower the required bandwidth and power consumption depending on the activity level of the test subject.

C. EKG

A power saving of 75% is realized by applying ADPCM to EKG signals (output from the signal generator) obtained at a rate of 200 12-bit samples/s. The normalized correlation of the received signal with respect to the autocorrelated input waveform is over 99%.

VI. Discussion

To put the system in perspective, we compare it with: 1) fully analog and 2) microcontroller-based solutions. The fully analog solutions do not provide onboard digital-signal processing or compression, and can, thus, be regarded as analog telemetry systems. However, these analog systems are only a fraction of the size and consume far less power than the system outlined in this paper. These analog systems also require custom receivers, and are not capable of communicating on any standard protocol (e.g., Health Level 7 [32]–[34], and IEEE [35]. Table I compares the key performance specifications of the system presented in this paper against those reported for several fully analog wireless biological signal-acquisition systems (covered in detail in [31]). The key parameters of interest are raw data throughput, range, power dissipation, size, and weight, as the fully analog nature of the integrated systems inhibits their ability to perform signal processing, although analog-domain signal processing is being investigated [30]. Table II compares the system presented in this paper with several recently reported microcontroller-based

wireless biological monitoring platforms. The system presented in [1] is an AMD-based 66-MHz PC-class device that communicates through an 802.11b wireless adapter. The system covered in [36] is a similar TelosB-based system that acquires ECG, yet does not perform onboard signal processing to lower power dissipation. The system covered in [15] is a PIC-enabled device that communicates over Bluetooth, which at a data transmission rate of 300 Hz, does not fully leverage the data throughput capability of its underlying hardware. The system covered in [17] is another Bluetooth-based system that acquires ECG, yet consumes power of the order of watts, as does [16], which is a PC-class device that communicates ECG over Bluetooth. Although all of the platforms compared in Table II could potentially provide a level of digital-signal processing capabilities, the computational capabilities of the microcontrollers have been solely used to implement communications protocols (e.g., Bluetooth, etc.), rather than biological-signal compression and interpretation (e.g., spike detection). Table II illustrates that the system reported in this paper provides similar signal-communications abilities (i.e., regarding channel count, data multiplexing, and standards-based communications protocols), while also demonstrating data compression and signal analysis, at a fraction of the size, weight, and power dissipation of the other reported microcontroller-based systems. An EKG monitor based on a TelosB mote [36], and a wireless pulse oximeter based on a MICA2 mote have been reported [20]; however, neither of these systems provide any onboard signal compression or event detection.

VII. Conclusion

In this paper, we have demonstrated an embedded sensor/system architecture for wireless biosignal recording. The wireless biological sensors leverage the limited signal-filtering capabilities of the COTS TelosB wireless-enabled processor modules on which they are based. By applying efficient filters, which were designed based on existing methods for interpreting biological signals, the power efficiency of the embedded system has been improved by a factor of over 400. After taking into account the standby power dissipation and communications-protocol overhead, a 360% improvement in battery life can be expected. Furthermore, onboard signal-processing capability has removed the bandwidth bottleneck imposed by the transceiver, thereby enabling signals to be sampled at double the rate at which they could be transmitted in raw form. Therefore, performing local signal processing not only lowers the power dissipated by the radio, but also enables the observer to sample data at rates that would be prohibitive if they were to be transmitted in raw format. We have demonstrated this by performing spike detection on data sampled at a rate of 8000 12-bit samples/s, which by no means could be supported by the radio. Two figures of merit have been introduced, i.e., ATEF for fully analog telemetry systems and DTEF for microcontroller-based telemetry systems. We calculated the ATEF and DTEF of our system, and compared it against those of several recently reported fully analog and microcontroller-based telemetry systems, respectively. The ATEF of the system presented in this paper is poor compared to the other fully analog telemetry systems, because it is significantly heavier and more power intensive. However, the DTEF of the system presented in this paper is orders-of-magnitude better than the microcontroller-based systems that have been reported in recent literature. For biomedical monitoring applications that require data rates of up to 32 kb/s, with the option of event detection, the system presented in this paper efficiently exploits an appropriate level of hardware capabilities.

Acknowledgment

The authors would like to thank Dr. A. Bragin for providing us with the raw neural recordings.

References

[1] I. Obeid, M. Nicolelis, and P. Wolf, "A multichannel telemetry system for single unit neural recordings," *J. Neurosci. Methods*, vol. 133, no. 1-2, pp. 33–38, 2004.

[2] P. Irazoqui-Pastor, I. Mody, and J. Judy, "Transcutaneous RF-powered neural recording device," in *Proc. 24th Annu. EMBS/BMES Conf. Eng. Med. Biol.* 2002, vol. 3, pp. 2105–2106

[3] S. Farshchi, A. Pesterev, P. Nuyujukian, I. Modi, and J. Judy, "A TinyOS-enabled MICA2-based wireless neural interface," *IEEE Trans. Biomed. Eng.*, vol. 53, no. 7, pp. 1416–1424, Jul. 2006.

[4] J. Hill, R. Szewczyk, A. Woo, S. Hollar, D. Culler, and K. Pister, "System architecture directions for network sensors," presented at ASPLOS, Cambridge, MA, Oct. 2000.

[5] S. Farshchi, P. Nuyujukian, A. Pesterev, I. Mody, and J. Judy, "A TinyOS-based wireless neural sensing, archiving, and hosting system," in *Proc. 2nd Int. IEEE EMBS Conf. Neural Eng.,* 2005, pp. 671–674.

[6] K. Wise, D. Anderson, J. Hetke, D. Kipke, and K. Najafi, "Wireless implantable microsystems: High-density electronic interfaces to the nervous system," *Proc. IEEE*, vol. 92, no. 1, pp. 76–97, Jan. 2004.

[7] C. Subbe, M. Kruger, P. Rutherford, and L. Gemmel, "Validation of a modified early warning score in medical admissions," *QJM*, vol. 94, pp. 521–526, 2001.

[8] H. Song, D. Allee, and K. Speed, "Single chip system for bio-data acquisition, digitization and telemetry," in *Proc. 1997 IEEE Int. Symp. Circuits Syst.*, Hong Kong, vol. 3, pp. 1848–1851.

[9] P. Mohseni, K. Najafi, and S. Eliades, "Wireless multichannel biopotential recording using an integrated FM telemetry circuit," *IEEE Trans. Neural Syst. Rehabil. Eng.*, vol. 13, no. 3, pp. 263–271, Sep. 2005.

[10] J. Parramon, P. Doguet, D. Marin, M. Verleyssen, R. Munoz, L. Leija, E. Valderrama, and B. Cnm, "ASIC-based batteryless implantable telemetry microsystem forrecording purposes," in *Proc. 19th Annu. Int. Conf. IEEE Eng. Med. Biol. Soc. 1997*, Chicago, IL, vol. 5, pp. 2225–2228

[11] A. Nieder, "Miniature stereo radio transmitter for simultaneous recording of multiple single-neuron signals from behaving owls," *J. Neurosci. Methods*, vol. 101, no. 2, pp. 157–64, 2000.

[12] S. Takeuchi and I. Shimoyama, "A three-dimensional shape memory alloy microelectrode with clipping structure for insect neural recording," *J. Microelectromech. Syst.*, vol. 9, no. 1, pp. 24–31, Feb. 2000.

[13] M. Modarreszadeh and R. Schmidt, "Wireless, 32-channel, EEG and epilepsy monitoring system," in *Proc. 19th Annu. Int. Conf. IEEE Eng. Med. Biol. Soc. 1997*, Chicago, IL, vol. 3, pp. 1157–1160

[14] I. Obeid and P. Wolf, "Evaluation of spike-detection algorithms fora brain-machine interface application," *IEEE Trans. Biomed. Eng.*, vol. 51, no. 6, pp. 905–911, Jun. 2004.

[15] C. Mundt, K. Montgomery, U. Udoh, V. Barker, G. Thonier, A. Tellier, R. Ricks, R. Darling, Y. Cagle, N. Cabrol *et al.*, "A multiparameter wearable physiologic monitoring system for space and terrestrial applications," *IEEE Trans. Inf. Technol. Biomed.*, vol. 9, no. 3, pp. 382–391, Sep. 2005.

[16] M. Rasid and B. Woodward, "Bluetooth telemedicine processor for multichannel biomedical signal transmission via mobile cellular networks," *IEEE Trans. Inf. Technol. Biomed.*, vol. 9, no. 1, pp. 35–43, Mar. 2005.

[17] J. Yao, R. Schmitz, and S. Warren, "A wearable point-of-care system for home use that incorporates plug-and-play and wireless standards," *IEEE Trans. Inf. Technol. Biomed.*, vol. 9, no. 3, pp. 363–371, Sep. 2005.

[18] B. Greenstein, A. Pesterev, C. Mar, E. Kohler, J. Judy, S. Farshchi, and D. Estrin, "Capturing high-frequency phenomena using a bandwidth-limited sensor network," in *Proc. ACM SenSys*, 2006.
[19] L. Girod, T. Stathopoulos, N. Ramanathan, J. Elson, D. Estrin, E. Osterweil, and T. Schoellhammer, "A system for simulation, emulation, and deployment of heterogeneous sensor networks," in *Proc. 2nd Int. Conf. Embedded Netw. Sensor Syst.*, 2004, pp. 201–213.
[20] K. Lorincz, D. Malan, T. Fulford-Jones, A. Nawoj, A. Clavel, V. Shnayder, G. Mainland, M. Welsh, and S. Moulton, "Sensor networks for emergency response: Challenges and opportunities," *IEEE Pervasive Comput.*, vol. 3, no. 4, pp. 16–23, Dec. 2004.
[21] M. Nicolelis, *Methods for Neural Ensemble Recordings*. Boca Raton, FL: CRC, 1999.
[22] M. Lewicki, "A review of methods for spike sorting: The detection and classification of neural action potentials," *Netw: Comput. Neural Syst.*, vol. 9, no. 4, pp. 53–78, 1998.
[23] R. Harrison, P. Watkins, R. Kier, R. Lovejoy, D. Black, R. Normann, and F. Solzbacher, "A low-power integrated circuit for a wireless 100-electrode neural recording system," in *IEEE ISSCC 2006 Tech. Dig.*, pp. 554–555.
[24] R. Harrison, "A low-power integrated circuit for adaptive detection of action potentials in noisy signals," in *Proc. 25th Annu. Int. Conf. IEEE EMBS*, 2003, pp. 3325–3328.
[25] P. Cummiskey, N. Jayant, and J. Flanagan, "Adaptive quantization in differential PCM coding of speech," *Bell Syst. Tech. J.*, vol. 52, no. 7, p. 1105, 1973.
[26] R. Jafari, H. Noshadi, M. Sarrafzadeh, and S. Ghiasi, "Adaptive medical feature extraction for resource constrained distributed embedded systems," in *Proc. 4th Annu. IEEE Int. Conf. Pervasive Comput. Commun. Workshops*, 2006, pp. 506–511.
[27] J. Pan and W. Tompkins, "A real-time QRS detection algorithm," *IEEE Trans. Biomed. Eng.*, vol. 32, no. 3, pp. 230–236, Mar. 1985.
[28] Y. Hu, W. Tompkins, J. Urrusti, and V. Afonso, "Applications of artificial neural networks for ECG signal detection and classification,," *J. Electrocardiol.*, vol. 26, pp. 66–73, 1993.
[29] G. Buzsaki, M. Penttonen, Z. Nadasdy, and A. Bragin, "Pattern and inhibition-dependent invasion of pyramidal cell dendrites by fast spikes in the hippocampus in vivo," *Proc. Nat. Sci. USA*, vol. 93, no. 18, pp. 9921–9925, 1996.
[30] P. Watkins, G. Santhanam, K. Shenoy, and R. Harrison, "Validation of adaptive threshold spike detector for neural recording," in *Proc. 26th Annu. Int. Conf. IEEE Eng. Med. Biol. Soc.*, 2004, vol. 2, pp. 4079–4082.
[31] S. Farshchi, W. Pesterev, A. Ho, I. Mody, and J. Judy, "Acquiring high-rate neural spike data with hardware-constrained embedded sensors," in *Proc. 28th Annu. Int. Conf. IEEE Eng. Med. Biol. Soc., 2006*, pp. 903–907.
[32] Hl7 United States. [Online]. Available: http://www.hl-7.org
[33] CEN/TC251-European standardization of health informatics. Nen-Dutch Standardization Inst. [Online]. Available: http://www.centc251.org
[34] Digital imaging and communications in medicine. Nat. Elect. Manuf. Assoc. [Online]. Available: http://medical.nema.org/dicom.html
[35] IEEE 1073 Gen. Committee. IEEE 1073 medical device communications. [Online]. Available: http://www.ieee1073.org
[36] T. Fulford-Jones, G. Wei, and M. Welsh, "A portable, low-power, wireless two-lead EKG system," in *Proc. 26th Annu. Int. Conf. IEEE Eng. Med. Biol. Soc.*, 2004, vol. 1, pp. 2141–2144.

Shahin Farshchi (S'03) was born in Berkeley, CA, in 1978. He received the B.S. (honors) degree in electrical engineering and computer science from the University of California, Berkeley, in 2002, and the M.S. and Ph.D. degrees in electrical engineering from the University of California, Los Angeles, in 2005 and 2006, respectively.

He is currently a Postdoctoral Fellow with the University of California, Los Angeles. His current research interests include developing wireless neural-signal acquisition, processing, and communications systems.

Aleksey Pesterev is currently working toward the B.S. degree in computer science and electrical engineering at the University of California, Los Angeles.

Paul H. Nuyujukian is currently working toward the B.S. degree in cybernetics at the University of California, Los Angeles.

Istvan Mody received the Ph.D. degree in physiology (neurophysiology) from the University of British Columbia, Vanouver, BC, Canada.

He was a Postdoctoral Researcher first with the Max-Planck Institute, Munich, Germany, and then with the Playfair Neuroscience Center, University of Toronto, Toronto, Ontario, ON, under an Izaak Walton Killam and a Canadian MRC Fellowhip. He was with the Department of Neurology and Neurological Sciences, Stanford University, California. He is currently the Tony Coelho Professor of Neurology and Professor of Physiology at the David Geffen School of Medicine, Department of Neurology, University of California, Los Angeles. His research interests include ligand-gated ion channels, inhibition in the brain, basic mechanisms of epilepsies, and the regulation of intraneural calcium.

Dr. Mody has recived several awards, including the Alfred Hauptmann Prize, the Michael Prize, the Basic Scientist Award from the AES/Milken Foundation, and the Javits Award from the National Institutes of Health/NINDS. He is a member of the Hungarian Academy of Sciences.

Jack W. Judy (S'87–M'96–SM'02) received the B.S.E.E. (*summa cum laude*) degree from the University of Minnesota, Minneapolis, in 1989, and the M.S. and Ph.D. degrees in electrical engineering from the University of California, Berkeley, in 1994 and 1996, respectively.

From 1996 to 1997, he was with Silicon Light Machines, Inc., Sunnyvale, CA. Since 1997, he has been a Faculty with the Department of Electrical Engineering, University of California, Los Angeles (UCLA), where he is currently an Associate Professor. At UCLA, he is the Chair of the MEMS and Nanotechnology Major Field of the Electrical Engineering Department and the Director of the UCLA NeuroEngineering Training Program. He is the Director of the UCLA Nanoelectronics Research Facility as well as the Director of the UCLA Microfabrication Laboratory. His research interests include novel ferromagnetic MEMS (e.g., MEMS magnetometers, reconfigurable frequency-selective surfaces, and implantable magnetic microactuators for biomedical applications), nanomagnetomechanical systems, chemical sensors, micromachined sensors for plasma research, wireless sensor networks, microprobes for Parkinson's disease research, implantable and flexible 3-D microelectrode arrays, dynamic modeling of 3-D microelectrodes, microelectrode arrays for high-density neural stimulation and retinal prostheses, simulation of the synthetic vision provided by retinal prostheses, micromachined systems to manipulate individual cells and to perform high-impedance patch-clamp recording, microactuators to solve the hydrocephalus shunt-clogging problem, wireless neural transceivers, brain–computer interfaces, and developing neural-control strategies and systems for functional deficits (e.g., spinal cord injury, ocular motility, and deep-brain stimulation). He has developed and improved graduate-level training programs in the multidisciplinary engineering fields of microelectromechanical systems, nanotechnology, and neuroengineering.